DOI: 10.1002/asia.200600070

A Myoglobin Functional Model Composed of a Ferrous Porphyrin and a Cyclodextrin Dimer with an Imidazole Linker

Koji Kano,*[a] Hiroaki Kitagishi,[a] Takahiro Mabuchi,[a] Masahito Kodera,[a] and Shun Hirota[b]

Abstract: A 1:1 inclusion complex (Fe^{II}PImCD) of 5,10,15,20-tetrakis-(4-sulfonatophenyl)porphinatoiron(II) (Fe^{II}P) and an O-methylated β-cyclodextrin dimer with an imidazole linker (ImCD) was found to bind dioxygen in aqueous solution. The half-saturation pressure of dioxygen ($P_{1/2}^{O2}$) is 1.7 torr at 25 °C, which is 10 times lower than that for a previous myoglobin functional model (hemoCD) with a pyridine linker. Meanwhile, the half-life of oxygenated Fe^{II}PImCD is 3 h, which is 10 times shorter than that of oxygenated hemoCD. The covering of the iron(II) center by a microscopic environment is essential for preventing autoxidation of oxygenated ferrous porphyrin, which is promoted by nucleophilic attack of H_2O and/or nucleophiles such as inorganic anions. Due to structural requirements, covering of the Fe^{II} center of Fe^{II}PImCD is insufficient compared with the case of hemoCD. As a result, water molecules can penetrate more easily the cleft of the O_2–Fe^{II}PImCD complex and act as an autoxidation inducer. This structure also causes poorer selectivity against carbon monoxide ($M = 1040$). In contrast, the dioxygen affinity of Fe^{II}PImCD is much higher than that of hemoCD because the imidazole moiety is a stronger electron donor than pyridine.

Keywords: carbonyl ligands · cyclodextrins · dioxygen ligands · heme proteins · imidazole

Introduction

The mimicking of the functions of hemoglobin (Hb) and myoglobin (Mb) in aqueous solution has been a longstanding problem.[1] A picket-fence porphyrin first reported by Collman et al. and its functionally similar compounds were prepared as models of Mb that work in absolute organic solvents such as toluene.[1–3] Although these Mb models have provided invaluable information on dioxygen binding to a ferrous porphyrin (Fe^{II}Por), the fundamental limitation is the solvent. Most models are effective only in absolute organic solvents. A trace amount of water causes autoxidation of the dioxygen adducts (O_2–Fe^{II}Por). Jiang and Aida studied the effect of water on the stability of O_2–Fe^{II}Por by using hydrophobic Fe^{II}Por dendrimers in water-saturated toluene.[4] Although a dioxygen adduct of the high-generation dendrimer is formed in water-saturated toluene, no information was derived about dioxygen binding in water because of the low solubility of the dendrimers. Similarly, Zingg et al. prepared water-soluble Fe^{II}Por dendrimers with polyoxyethylene chains.[5] Such dendrimers form very stable dioxygen adducts in absolute toluene ($P_{1/2}^{O_2} = 0.035$–0.016 torr; $P_{1/2}^{O_2}$ represents the partial dioxygen pressure at which half of the Fe^{II}Por molecules are oxygenated), but not in water-saturated toluene. No dioxygen adduct is formed in water. The protoporphyrin IX moiety in Hb or Mb is located near the surface of the protein globin.[6,7] However, autoxidation in biological systems proceeds very slowly.[8] It may be important to place the Fe^{II} center at a microscopically hydrophobic environment from which water molecules are strictly excluded. Tsuchida and co-workers proved this assumption by studying dioxygen binding to hydrophobic or amphiphilic Fe^{II}Pors in hydrophobic environments such as liposomal membranes or albumin in aqueous solutions.[9–11]

Cyclodextrins (CDs) are unique host molecules that include various hydrophobic chemical species into their hydrophobic cavities in aqueous solution.[12–14] This characteristic of CDs has been utilized to prepare enzyme models.[12–14] Investigations on interactions of water-soluble porphyrins with

[a] Prof. K. Kano, Dr. H. Kitagishi, T. Mabuchi, Prof. M. Kodera
Department of Molecular Science and Technology
Faculty of Engineering, Doshisha University
Kyotanabe, Kyoto 610-0321 (Japan)
Fax: (+81) 774-65-6845
E-mail: kkano@mail.doshisha.ac.jp

[b] Dr. S. Hirota
Kyoto Pharmaceutical University
Yamashina-ku, Kyoto 607-8414 (Japan)

Supporting information for this article is available on the WWW under http://www.chemasianj.org or from the author.

CDs have been carried out in connection with metalloenzymes.[15–17] Komatsu et al. reported dioxygen binding to a ferrous complex of a tetracationic picket-fence porphyrin whose iron center was coordinated by an imidazole derivative incorporated into an α-CD cavity in DMF/H_2O (3:2; DMF = *N*,*N*-dimethylformamide).[18] They showed the UV/Vis spectra of oxygenated Fe^{II}Por and carbon monoxide coordinated Fe^{II}Por as the only evidence for formation of the dioxygen adduct. Our experience, however, questions the solvent used in this study. DMF usually contains some amine(s) as impurity, which can reduce Fe^{III}Por to Fe^{II}Por. Therefore, the formation of CO-coordinated Fe^{II}Por might not be evidence of the dioxygen adduct as a precursor of CO–Fe^{II}Por in a solution containing DMF. Zhou and Groves reported a Mb functional model composed of a water-soluble Fe^{II}Por and a CD with polyoxyethylene tails and a tail containing a pyridine moiety.[19] Such a system is mysterious because the oxygenated Fe^{II}Por is fairly stable in spite of the fluctuant and somewhat hydrophilic nature of the polyoxyethylene chains. Previous studies revealed that O_2–Fe^{II}Por is easily autoxidized to a superoxide anion and Fe^{III}Por by water.[4,5,8] Recently, we developed a Mb (Hb) functional model (hemoCD) composed of an O-methylated β-cyclodextrin dimer with a pyridine linker (PyCD, Py = pyridine) and 5,10,15,20-tetrakis(4-sulfonatophenyl)porphinato iron(II) (Fe^{II}P) (Figure 1).[20] HemoCD shows a moderate dioxygen affinity ($P_{1/2}^{O_2}$ = 16.9 torr in phosphate buffer at pH 7.0 and 25 °C) and its dioxygen adduct (oxyhemoCD) has a long half-life ($t_{1/2}$ = 30 h). Although hemoCD is an excellent functional model of Mb (Hb) in aqueous solution, a pyridine moiety is used as the axial ligand, whereas the imidazole moiety of a histidine (His) residue acts as a proximal base that stabilizes oxyMb or oxyHb. Imidazole is a stronger base than pyridine; it thus participates in stronger back-bonding from Fe^{II} to the bound dioxygen to strengthen the Fe–O_2 bond.[21,22] It can be expected, therefore, that replacement of the pyridine linker of hemoCD by an imidazole linker would improve the ability of the model to bind dioxygen in aqueous solution. Herein, we prepared an O-methylated β-CD dimer that bears an imidazole linker (ImCD, Im = imidazole; Figure 1) and found that a 1:1 inclusion complex of ImCD and Fe^{II}P (Fe^{II}PImCD) showed a higher and lower ability to bind dioxygen and carbon monoxide, respectively, in aqueous solution than the pyridine analogue.

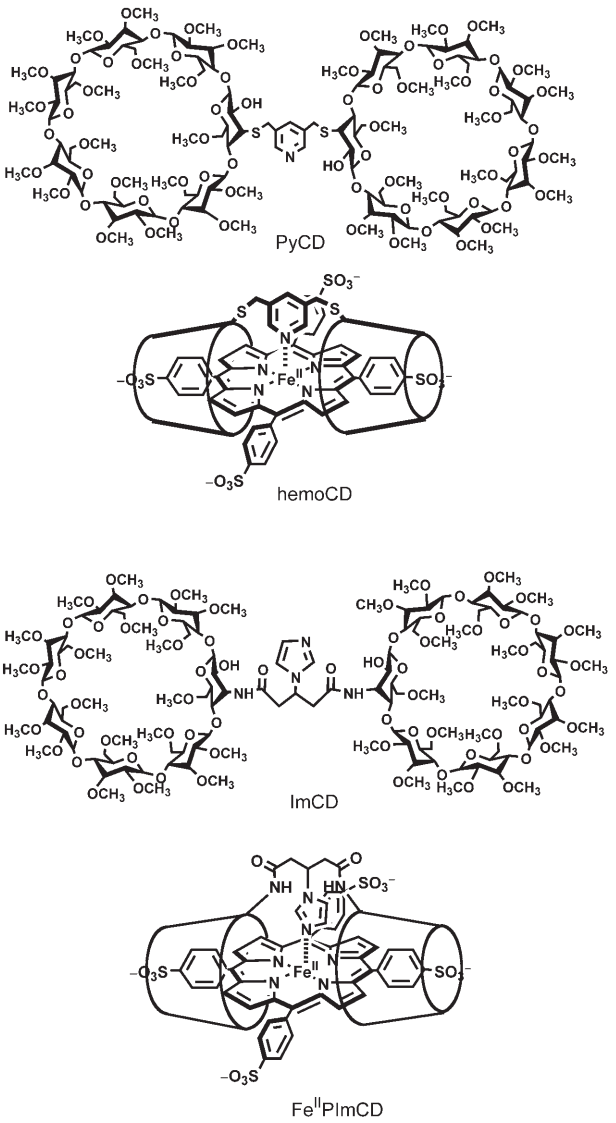

Figure 1. Structures of hemoCD (composed of PyCD and Fe^{II}P) and Fe^{II}PImCD (composed of ImCD and Fe^{II}P).

Results and Discussion

Preparation of ImCD

The synthesis of ImCD was performed according to the procedure shown in Scheme 1. The point of this synthesis is the O-methylation of mono(2^A,3^A-epoxy)-β-CD (EpoCD). Previously, we found that heptakis(2,3,6-tri-*O*-methyl)-β-cyclodextrin (TMe-β-CD) forms extremely stable 2:1 inclusion complexes with 5,10,15,20-tetrakis(4-sulfonatophenyl)porphyrin (tpps) and its Fe^{III} complex (Fe^{III}P) in aqueous solution.[17] Therefore, the O-methylation is essential in this study. Another point is the nucleophilic attack of ammonia on EpoCD to afford NH_2-CD. An amino group is selectively attached to the 3-position of the O-methylated glucopyranose.[20] The following condensation with 3-(1H-imidazol-1-yl)pentanedioic acid using HOBt (1-hydroxy-1H-benzotriazole) and DCC (*N*,*N*′-dicyclohexylcarbodiimide) as the condensation agents, therefore, affords the CD dimer linked at the 3-positions of the CD molecules. To increase the yield of ImCD, the isolation procedure should be improved upon; strong adsorption of polar ImCD on silica gel during purification reduced the yield of ImCD.

Complexation of ImCD with Tpps and Fe^{III}P

At first, complexation of free base tpps with ImCD was investigated to obtain basic information about complexation of ImCD with porphyrins. Figure 2 shows the UV/Vis spec-

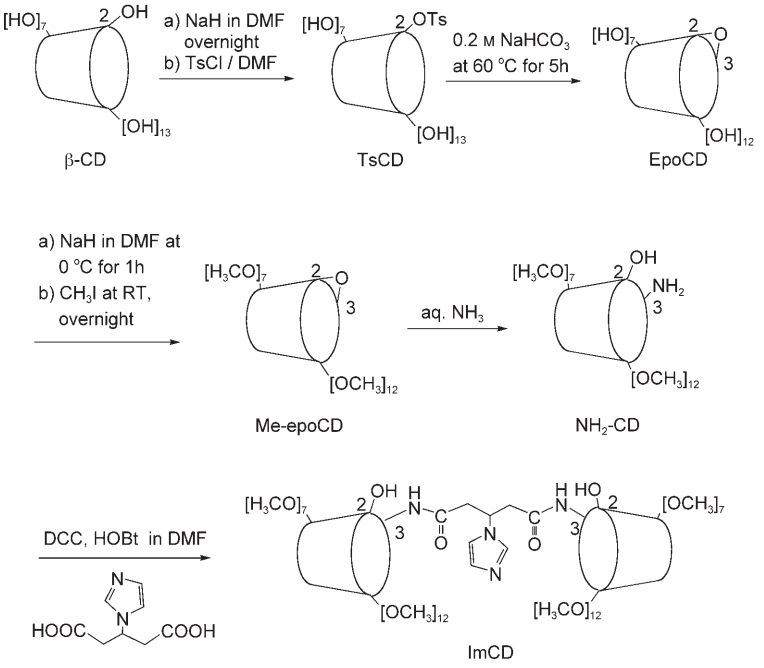

Scheme 1. Synthetic route to ImCD. Bt = 1-benzotriazolyl, DCC = *N*,*N*′-dicyclohexylcarbodiimide, Ts = *p*-toluenesulfonyl.

tral changes of tpps upon addition of ImCD. These changes clearly reached a plateau after the addition of one equivalent of ImCD, thus indicating the formation of a very stable 1:1 complex of tpps and ImCD.

We have often used the pK_a value of diprotonated free base porphyrin to evaluate the hydrophobicity at the center of the porphyrin sandwiched by two CD cavities.[17a,23] The intensity of the Soret band of free base tpps at 415 nm decreased with decreasing pH, and a new band due to diprotonated tpps appeared at 433 nm together with isosbestic points (Supporting Information). As shown in Table 1, the pK_a value of the tpps–ImCD complex was determined to be

Table 1. The pK_a values of diprotonated tpps in aqueous solution in the absence and presence of CDs at 25 °C.

CD	pK_a	ΔpK_a	Reference	CD	pK_a	ΔpK_a	Reference
none	4.8	0	[24]	PyCD	<0.3	>4.5	[23]
β-CD	4.2	0.6	[17a]	ImCD	2.7	2.1	this work
TMe-β-CD	0.4	4.4	[17a]				

2.7, which is much larger than those of the 1:2 complex of tpps and TMe-β-CD (0.4) and the 1:1 complex of tpps and PyCD (<0.3), thus suggesting that the cleft formed by the two CD moieties of the tpps–ImCD complex is wider than those of tpps–TMe-β-CD and tpps–PyCD. As a consequence, the microscopic environment at the porphyrin center of the tpps–ImCD complex may be more hydrophilic than that of tpps–TMe-β-CD and tpps–PyCD. The imidazole moiety is bound to the CD cavities by amide linkages, which are less flexible than the thioether linkages of PyCD. Therefore, the two CD moieties of ImCD may not be close to each other.

$Fe^{III}P$ also forms a very stable 1:1 complex with ImCD (Fe^{III}PImCD), as revealed by UV/Vis spectroscopy (Supporting Information). At pH 7.0, $Fe^{III}P$ exists as a μ-oxo dimer. Upon addition of ImCD, the μ-oxo dimer with λ_{max} at 408 nm dissociated to the 1:1 complex of $Fe^{III}P$ and ImCD with λ_{max} at 416 nm. The fact that inclusion of $Fe^{III}P$ into the cavities of ImCD completely inhibits the formation of the μ-oxo dimer is important in the construction of a Mb or Hb model in aqueous solution.[16c,17c,25]

The next problem is the ligation of the imidazole moiety to the iron atom of the porphyrin. Since $Fe^{II}P$ is unstable in aerobic solution, we used $Zn^{II}P$ in

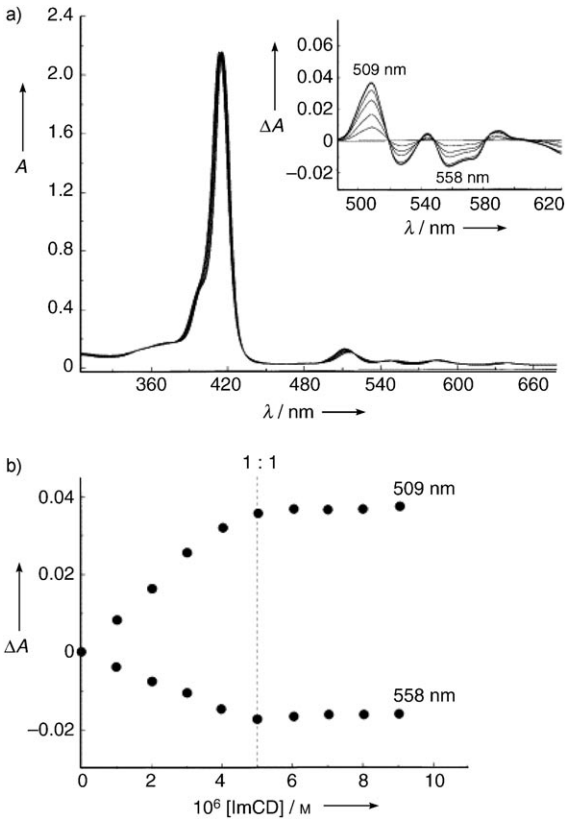

Figure 2. a) UV/Vis spectral changes of tpps (5×10^{-6} M) in phosphate buffer (0.05 M) at pH 7.0 and 25 °C upon addition of ImCD. The inset shows the difference spectra. b) Plot of the change in absorbance of tpps versus [ImCD].

CHEMISTRY
AN ASIAN JOURNAL

place of the ferrous complex. UV/Vis spectroscopy indicated the formation of an extremely stable 1:1 complex of $Zn^{II}P$ and ImCD (Supporting Information). The pH-dependent absorption spectra of $Zn^{II}PImCD$ are shown in Figure 3.

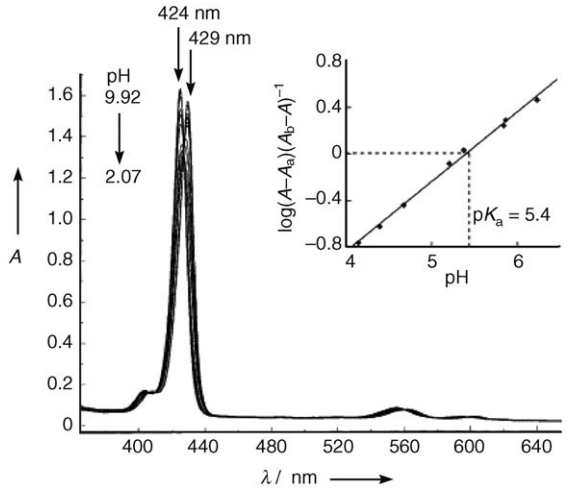

Figure 3. UV/Vis spectral changes of $Zn^{II}P$ (4×10^{-6} M) complexed with ImCD (4.8×10^{-6} M) as a function of pH in aqueous $NaClO_4$ (0.1 M) at 25 °C. The pH values were adjusted by NaOH and $HClO_4$. The inset shows the plot of $\log(A-A_a)(A_b-A)^{-1}$ at 424 nm versus pH for determining the pK_a value of the protonated ImCD.

The pH titration curve suggests a pK_a value of 5.4 that corresponds to dissociation of the coordination bond between Zn^{II} and the imidazole nitrogen atom due to protonation of imidazole. The pK_a value of 1-methylimizadole is 7.33;[26] the discrepancy in pK_a values may be ascribed to the hiding of the imidazole moiety in the cleft of the ImCD dimer. On the basis of these data, it is reasonable to assume that imidazole coordinates to the $Fe^{II}PImCD$ complex in aqueous solution at pH 7.0.

Dioxygen Binding

$Fe^{III}PImCD$ in Ar-saturated phosphate buffer at pH 7.0 was reduced by two equivalents of $Na_2S_2O_4$ to prepare a stock solution of $Fe^{II}PImCD$, which was diluted by phosphate buffer at pH 7.0 under N_2 atmosphere. The resulting solution showed λ_{max} at 434 nm ($\varepsilon=2.33\times10^5\,M^{-1}cm^{-1}$) (Figure 4). At this stage, no absorption band due to $Na_2S_2O_4$ was detected. Dioxygen gas was then bubbled into the solution to afford the oxygenated $Fe^{II}PImCD$. The absorption maximum of the O_2 adduct of $Fe^{II}PImCD$ was observed at 423 nm ($\varepsilon=1.57\times10^5\,M^{-1}cm^{-1}$), which is in good agreement with the λ_{max} value of oxyhemoCD.[20] Introduction of CO gas into the solution of O_2 adduct caused the spectral peak to sharpen and enlarge ($\lambda_{max}=424$ nm, $\varepsilon=3.12\times10^5\,M^{-1}cm^{-1}$), thus indicating the formation of CO-coordinated $Fe^{II}PImCD$. This means that the absorption spectrum of the oxygenated sample is not due to $Fe^{III}PImCD$ formed by autoxidation. However, as the UV/Vis spectrum of $Fe^{III}PImCD$ is similar to that of O_2–$Fe^{II}PImCD$, further evidence should be obtained to prove the formation of O_2–$Fe^{II}PImCD$.

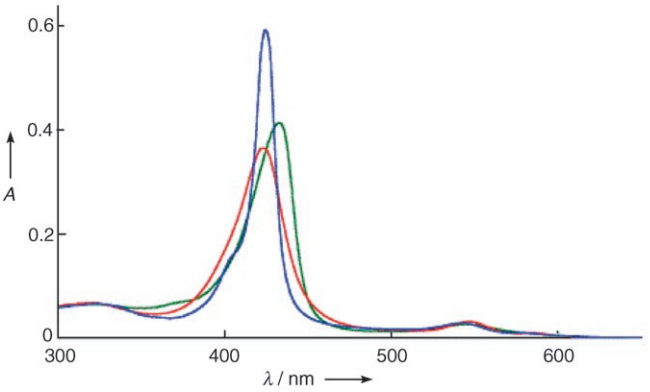

Figure 4. UV/Vis spectra of $Fe^{II}PImCD$ in the deoxy form (green) as well as the O_2-coordinated (red) and CO-coordinated forms (purple) in phosphate buffer (0.05 M) at pH 7.0 and 25 °C. The method of sample preparation is given in the text.

As five-coordinate $Fe^{II}PImCD$ is in a high-spin state ($S=2$), this compound shows ^1H NMR signals in the paramagnetic region.[27] As shown in Figure 5, the signals due to the

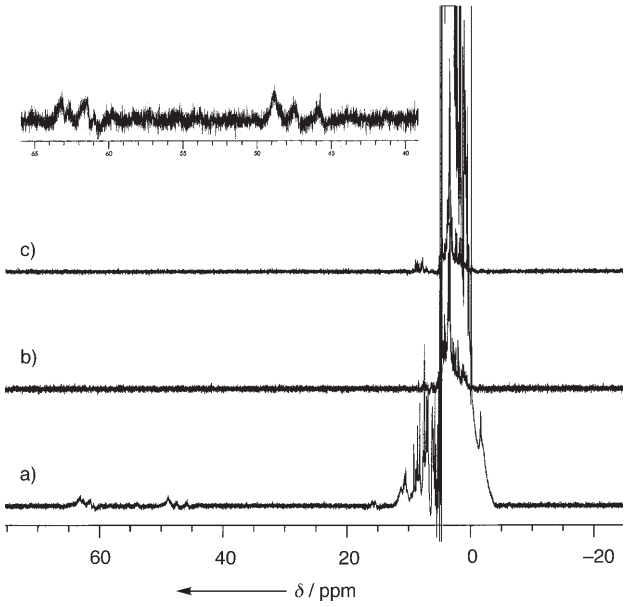

Figure 5. ^1H NMR spectra of a) $Fe^{II}PImCD$, b) O_2–$Fe^{II}PImCD$, and c) CO–$Fe^{II}PImCD$ in phosphate buffer (0.05 M, D_2O) at pD 7.0 and 25 °C. The inset shows a selected region (40–65 ppm) of spectrum a).

β protons of the pyrrole moiety of $Fe^{II}PImCD$ were observed in the region between 45 and 65 ppm. On the other hand, all the signals of oxygenated $Fe^{II}PImCD$ appeared in the region between 0 and 10 ppm, which indicates the formation of the six-coordinate diamagnetic O_2–$Fe^{II}PImCD$. Similarly, signals in the diamagnetic region were also observed for the CO-coordinated complex.

Resonance Raman spectroscopy is a powerful tool for studying gaseous ligation to metal complexes.[28] The reso-

nance Raman spectra of Fe^{II}PImCD in $^{16}O_2$ and $^{18}O_2$ atmospheres are shown in Figure 6. The isotope effect on the Raman peak means that the peak at 573 cm^{-1} for $^{16}O_2$ is ascribed to the stretching of the Fe–O_2 bond. The ν_{Fe-O2} frequency for O_2–Fe^{II}PImCD is in good agreement with that for sperm whale Mb (Table 2). On the other hand, the ν_{Fe-O2} frequency for O_2–Fe^{II}PImCD is 4 cm^{-1} higher than that for oxyhemoCD,[20] which suggests that the Fe–O_2 bond of O_2–Fe^{II}PImCD is stronger than that of oxyhemoCD. A similar result was obtained for the model system in toluene.[22] All spectroscopic results clearly indicate the formation of O_2–Fe^{II}PImCD with a relatively strong Fe–O_2 bond in aqueous solution.

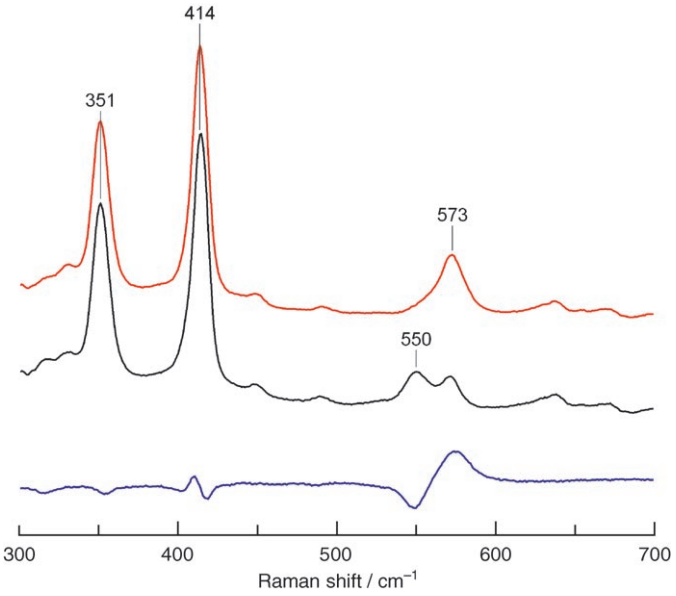

Figure 6. Resonance Raman spectra of the $^{16}O_2$ (red) and $^{18}O_2$ (black) adducts of Fe^{II}PImCD and the difference spectrum (purple). Experimental conditions: phosphate buffer (0.05 M) at pH 7.0, room temperature, 413.1 nm excitation, 5 mW power.

Table 2. Fe–O_2 (ν_{Fe-O2}), Fe–CO (ν_{Fe-CO}), and C–O stretching frequencies (ν_{C-O}) of myoglobin, hemoglobin, and model complexes.

Complex	ν_{Fe-O2} [cm^{-1}]	ν_{Fe-CO} [cm^{-1}]	ν_{C-O} [cm^{-1}]	Solvent
Mb (sperm whale)	573[28b]	507[29]	1947[29]	H_2O
Mb (horse)	571[28c]			H_2O
Hb (human)	568[28c]	507[29]	1951[29]	H_2O
Fe^{II}(TpivPP)(1-MeIm)[a]	571[28d]	489[29]	1969[29]	benzene
Fe^{II}tpp(1,2-Me_2Im)[29][b]		494	1972	benzene
Fe^{II}tpp(Py)[29]		484	1976	benzene
Fe^{II}tpps(2-MeIm)[29]		489	1972	H_2O
TCP–Im[c]	586	470	1994	toluene
TCP–Py[c]	583	465	2008	toluene
hemoCD	569[20]	480[23]	1987[23]	H_2O
Fe^{II}PImCD	573	487	1982	H_2O

[a] Fe(TpivPP) = *meso*-5α,10α,15α,20α-tetrakis(*o*-pivalamidophenyl)porphyrinatoiron. [b] tpp = 5,10,15,20-Tetrakis(4-sulfonatophenyl)porphyrin dianion. [c] TCP–Im and TCP–Py = iron(II) complexes of tetraphenylporphyrin derivative whose 2′- and 6′-positions of the phenyl groups are substituted by binaphthyl derivatives (Registry Number: 7439-89-6).[22]

The dioxygen affinity of an O_2 receptor is given by $P_{1/2}^{O_2}$, the partial pressure of dioxygen at which half of the receptor molecules forms the dioxygen adduct [Eq. (1)].

$$P_{1/2}^{O_2} = [Fe^{II}PImCD]P^{O_2}/[O_2 - Fe^{II}PImCD] \quad (1)$$

From this equation, Equation (2) can be derived to determine $P_{1/2}^{O_2}$ experimentally:

$$P^{O_2} = \{\Delta\varepsilon[Fe^{II}PImCD]_0 P^{O_2}\}/\Delta A - P_{1/2}^{O_2} \quad (2)$$

where $\Delta\varepsilon$ and ΔA are the differences in the extinction coefficients and the absorbances, respectively, between O_2–Fe^{II}PImCD and Fe^{II}PImCD at a certain wavelength, and $[Fe^{II}PImCD]_0$ is the initial concentration of Fe^{II}PImCD. $P_{1/2}^{O_2}$ can be determined from the vertical intercept of the straight line plot of P^{O_2} versus $P^{O_2}/\Delta A$. The UV/Vis absorption spectra of Fe^{II}PImCD at various P^{O_2} values and the plot of P^{O_2} versus $P^{O_2}/\Delta A$ are shown in Figure 7. The $P_{1/2}^{O_2}$ value

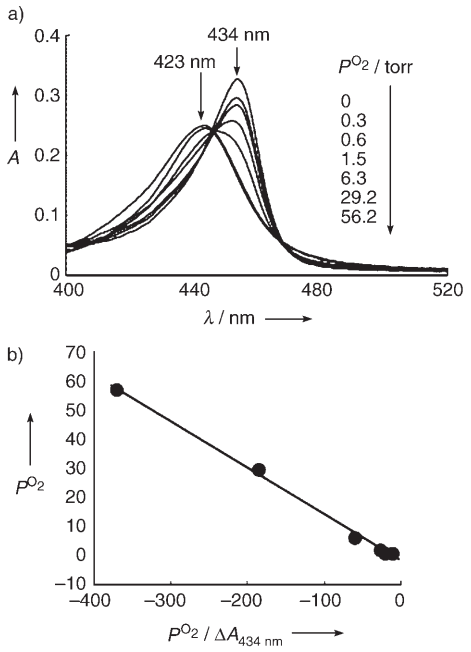

Figure 7. a) UV/Vis spectral changes of Fe^{II}PImCD in phosphate buffer (0.05 M) at pH 7.0 and 25 °C as a function of P^{O_2} in N_2. b) Plot of $P^{O_2}/\Delta A_{434\ nm}$ versus P^{O_2} for determining $P_{1/2}^{O_2}$ [Eq. (2)].

of Fe^{II}PImCD was determined to be 1.7 torr in phosphate buffer at pH 7.0 and 25 °C, that is, 10 times smaller than that of hemoCD (Table 3). As expected, coordination of the imidazole moiety to Fe^{II}P caused marked enhancement of the dioxygen affinity relative to pyridine coordination.

The dioxygen adduct of Fe^{II}PImCD was gradually autoxidized to Fe^{III}PImCD (Supporting Information), and the pseudo-first-order rate constant (k_{obs}) and the half-life ($t_{1/2}$) of O_2–Fe^{II}PImCD in phosphate buffer at pH 7.0 and 25 °C

Table 3. Affinities for O_2 and CO binding in biological and model systems.

System	$P_{1/2}^{O_2}$ [torr]	$P_{1/2}^{CO}$ [torr]	M[a]	Reference
Mb (sperm whale)	0.54[b]	0.029[b]	18.6	[30]
Mb (human)	0.69	0.023	30	[30]
Hb (human, R state)	0.22	1.3×10^{-3}	150	[1a]
$FePiv_3$5CIm[c]	0.58	2.2×10^{-5}	26600	[31]
Fe(PF3CUIm)[c]	1.26	4.9×10^{-5}	26000	[21]
Fe(PF3CUPy)[c]	52.2	6.4×10^{-4}	76000	[21]
TCP–Im[c]	1.3	1.1×10^{-3}	1180	[22]
TCP–Py[c]	9.4	1.7×10^{-2}	550	[22]
hemoCD	16.9	1.5×10^{-5}	1.1×10^{6}	[23]
Fe^{II}PImCD	1.7	1.6×10^{-3}	1040	this work

[a] M is given by [Eq. (4)]. [b] These values were calculated from K values reported in reference [30]. [c] $FePiv_3$5CIm = *meso*-5α,10α,15α-tris(*o*-pivalamidophenyl)-20β-{*o*-[5-(*N*-imidazolyl)valeramido]phenyl}porphyrinatoiron, Fe(PF3CUIm) = *meso*-5α,10α,15α-tris(*o*-pivalamidophenyl)-20β-{*o*-{[3-(*N*-imidazolyl)propyl]ureido}phenyl}porphyrinatoiron, Fe(PF3CUPy) = *meso*-5α,10α,15α-tris(*o*-pivalamidophenyl)-20β-{*o*-{[3-(3-pyridyl)propyl]ureido}phenyl}porphyrinatoiron, TCP–Im and TCP–Py = iron(II) complexes of tetraphenylporphyrin derivative whose 2′- and 6′-positions of the phenyl groups are substituted by naphthyl derivatives (Registry Number: 7439-89-6). The experiments of these model compounds were carried out in absolute toluene.

were 0.19 h^{-1} and 3.6 h, respectively. O_2–Fe^{II}PImCD is considerably less stable than oxyhemoCD ($t_{1/2}$ = 30 h).[20] There is an inconsistency in the stability of O_2–Fe^{II}PIm, namely, the dioxygen adduct of Fe^{II}PImCD is less stable than oxyhemoCD, even though its Fe^{II}–O_2 bond is stronger than that of oxyhemoCD, as suggested by the resonance Raman spectra. The mechanism for autoxidation of oxyMb and oxyHb is not well-understood.[1a,8,23] Shikama demonstrated that the water molecule acts as a nucleophile in the autoxidation of oxyMb, in which H_2O attacks the Fe^{II}–O_2 bond to yield metMb (metMb = ferric myoglobin) and O_2^-.[8] In a previous paper,[23] we verified the water-promoted autoxidation of oxyhemoCD as that shown in Equation (3).

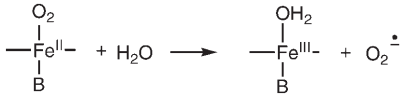

(3)

As suggested by the pK_a value of the tpps–ImCD complex, the cleft of Fe^{II}PImCD is wider than that of hemoCD. Therefore, the water molecules may penetrate the cleft of O_2–Fe^{II}PImCD more easily than in the case of oxyhemoCD, thus leading to faster autoxidation. The autoxidation of O_2–Fe^{II}PImCD promoted by water molecules seems to shorten its lifetime.

In the case of oxyhemoCD, dilution of gaseous O_2 by N_2 causes dissociation of bound dioxygen to yield hemoCD without change in the valency of the iron ion. This means reversible dioxygen binding in the hemoCD system. For O_2–Fe^{II}PImCD, however, bubbling of N_2 gas into the solution of O_2–Fe^{II}PImCD led to autoxidation, and no reversibility was observed. This result is also interpreted in terms of the wider cleft of the O_2–Fe^{II}PImCD complex leading to faster autoxidation.

Carbon Monoxide Binding

Carbon monoxide is a stronger ligand than dioxygen, and bound dioxygen is usually replaced by CO upon exposure to an atmosphere containing CO. The O_2/CO selectivity of the system is given by M in Equation (4):

$$M = P_{1/2}^{O_2}/P_{1/2}^{CO} = \{[CO - Fe^{II}PImCD]P^{O2}\}/\{[O_2 - Fe^{II}PImCD]P^{CO}\} \quad (4)$$

where $P_{1/2}^{CO}$ is given by Equation (5):

$$P_{1/2}^{CO} = \{[Fe^{II}PImCD]P^{CO}\}/[CO - Fe^{II}PImCD] \quad (5)$$

After the UV/Vis spectra of a solution of O_2–Fe^{II}PImCD was recorded for determining $P_{1/2}^{O2}$, the spectral changes were taken upon exposing the solution to atmospheres with various partial pressures of carbon monoxide in dioxygen (Figure 8). Under such conditions, P^{CO} can be represented by Equation (6):

$$P^{CO} = \{\Delta\varepsilon'[O_2 - Fe^{II}PImCD]_0P^{CO}\}/\Delta A' - P'_{1/2}{}^{CO} \quad (6)$$

where $\Delta\varepsilon'$ and $\Delta A'$ represent the differences in the extinction coefficients and the absorbances, respectively, between CO–Fe^{II}PImCD and O_2–Fe^{II}PImCD at a certain wavelength, and $[O_2$–$Fe^{II}PImCD]_0$ is the initial concentration of O_2–Fe^{II}PImCD. The linear relationship between P^{CO} and $P^{CO}/\Delta A'$ gave the $P'_{1/2}{}^{CO}$ value of 0.73 torr in the O_2/CO mixed atmosphere. The $P'_{1/2}{}^{CO}$ value corresponds to the CO partial pressure when $[O_2$–$Fe^{II}PImCD] = [CO$–$Fe^{II}PImCD]$. As P^{O2} under these conditions was 759.27 torr, M was found to be

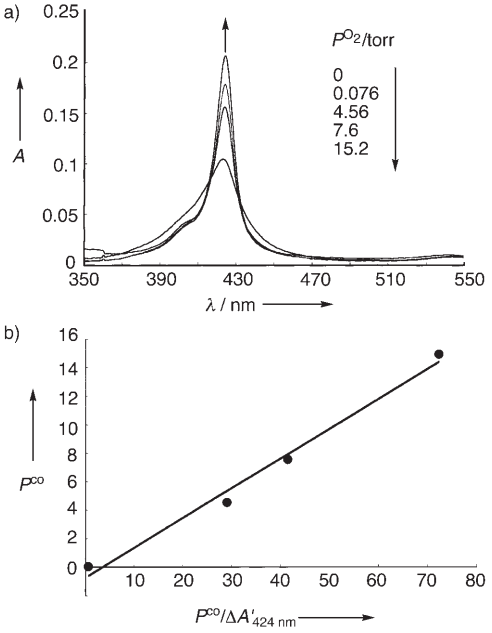

Figure 8. a) UV/Vis spectral changes of O_2–Fe^{II}PImCD in phosphate buffer (0.05 M) at pH 7.0 and 25 °C as a function of P^{CO} in O_2. b) Plot of $P^{CO}/\Delta A'_{434\,nm}$ versus P^{CO} for determining $P'_{1/2}{}^{CO}$ [Eq. (6)].

1040. Thus, $P_{1/2}^{CO}$ as defined by Equation (5) was calculated from Equation (4) to be 1.6×10^{-3} torr. The $P_{1/2}^{CO}$ and M values for the hemoCD system are 1.5×10^{-5} torr and 1.1×10^{6}, respectively.[20] The present system shows significantly poorer selectivity for CO compared with the hemoCD as well as picket-fence porphyrin systems (Table 3).

To investigate the poor CO selectivity of the present system, resonance Raman spectra of CO–Fe^{II}PImCD were measured. The results are shown in Figure 9. The assignment of the resonance Raman peaks was carried out according to isotope effects by using $^{12}C^{16}O$ and $^{13}C^{18}O$. The difference spectra clearly indicate that the peaks at 487 and 475 cm^{-1} arise from the stretching (ν_{Fe-CO}) of the Fe–$^{12}C^{16}O$ and Fe–$^{13}C^{18}O$ bonds, respectively, and that those at 1982 and 1890 cm^{-1} are the ν_{C-O} stretching bands of ^{12}C–^{16}O and ^{13}C–^{18}O, respectively, bound to Fe^{II}P. As no Fe–C–O bending mode was detected, the CO molecule seems to take on a linear geometry in the CO complex of Fe^{II}PImCD.

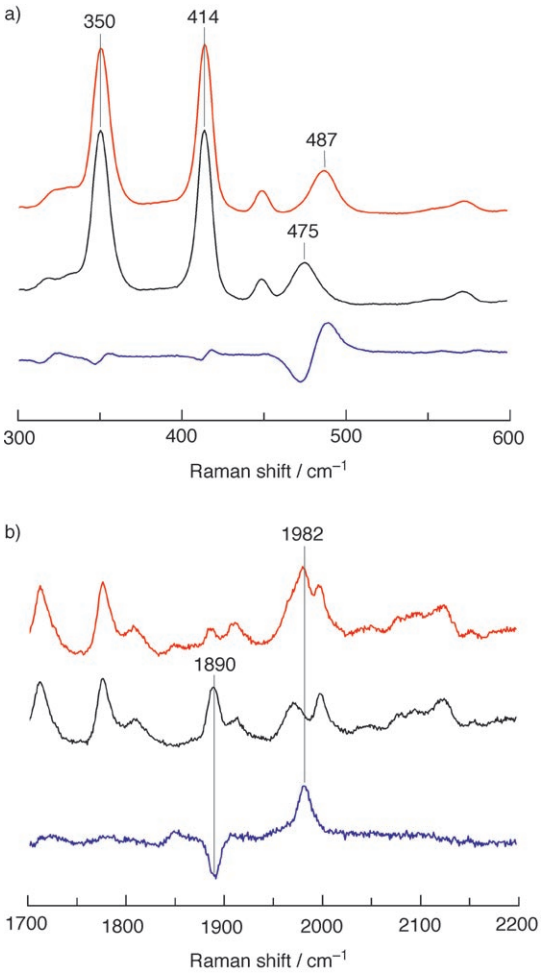

Figure 9. Resonance Raman spectra in the a) 300–600 cm^{-1} and b) 1700–2200 cm^{-1} regions of the $^{12}C^{16}O$ (red) and $^{13}C^{18}O$ adducts (black) of Fe^{II}PImCD in phosphate buffer (0.05 M) at pH 7.0 and room temperature, and their difference spectra (purple). The sample was irradiated by laser light of 413.1 nm at 5 mW power.

A negative correlation has been found between ν_{Fe-CO} and ν_{CO} in the complexation of natural hemoproteins and their mutants and model ferrous complexes with carbon monoxide (Figure 10).[28a,29,32] The ν_{Fe-CO} and ν_{CO} bands are known to shift to lower and higher wavenumbers, respectively, with decreasing strength of the Fe–CO bond.[28a,29,32] The plots of ν_{Fe-CO} versus ν_{CO} for CO–Fe^{II}PImCD and CO–hemoCD are shown in Figure 10. In both cases, they appear on the right, which suggests that the Fe^{II}–CO bonds in CO–Fe^{II}PImCD and CO–hemoCD are weak. In the case of CO–hemoCD, the $P_{1/2}^{CO}$ and M values are 1.5×10^{-5} torr and 1.1×10^{6}, respectively. Such novel CO selectivity of hemoCD is explained by the capping effect of the two cyclodextrin moieties that cover the Fe^{II} center of the porphyrin, leading to a cage. There, the pair of dissociated CO and deoxyhemoCD is equivalent to CO-bound hemoCD.[23] Meanwhile, the CO molecule dissociated from CO–Fe^{II}PImCD may diffuse to the aqueous bulk phase more easily than in the case of hemoCD, because capping by the cyclodextrin moieties of the present system is looser than that in the hemoCD system.

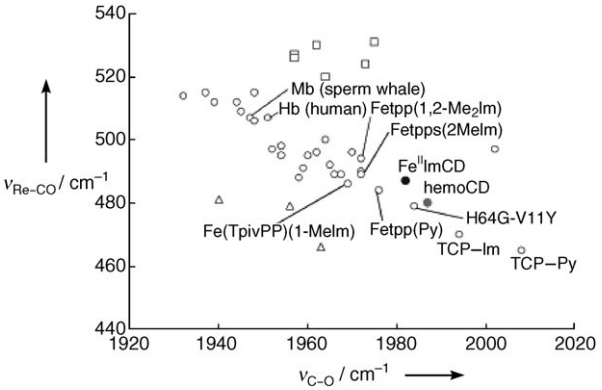

Figure 10. Plot of ν_{Fe-CO} versus ν_{C-O} for the CO complexes of the native, mutated, and model systems. All data points except for the TCP–Py, TCP–Im,[22] hemoCD, and Fe^{II}PImCD systems are quoted from reference [29]. ○ = Nitrogen-ligated heme systems, △ = thiolate-ligated heme systems, □ = heme systems with weak or absent proximal ligands.

Olson and co-workers[33] as well as Tani, Naruta, and co-workers[22,32] claimed a "negative polar effect" on the destabilization of CO-bound ferrous porphyrins. Back-bonding from Fe^{II} to CO enhances the double-bond nature of the Fe^{II}–CO bond and strengthens it. Meanwhile, the negative polar environment around the bound CO depresses the back-bonding to weaken that bond. For both CO–Fe^{II}PImCD and CO–hemoCD, the Fe^{II}–CO bond is surrounded by 24 OCH_3 and two OH groups. Therefore, the Fe^{II}–CO bonds in CO–Fe^{II}PImCD and CO–hemoCD are in an extremely polar environment and are thus very weak.

The ν_{Fe-CO} and ν_{CO} peaks in the resonance Raman spectra of CO–Fe^{II}PImCD appeared at higher and lower wavenumbers, respectively, than those of CO–hemoCD. Therefore,

CHEMISTRY
AN ASIAN JOURNAL

the Fe^{II}–CO bond of CO–Fe^{II}PImCD seems to be stronger than that of CO–hemoCD. This result is interpreted in terms of the stronger electron-donating ability of the imidazole moiety than that of the pyridine and instantly supports the cage effect on the stabilization of CO–hemoCD.

Energy-Minimized Structure of Fe^{II}PImCD

We assumed that the difference in O_2- and CO-binding behavior between Fe^{II}PImCD and hemoCD is mainly ascribed to the difference in the degree of encapsulation of Fe^{II}P by the two cyclodextrin moieties. To confirm that the cleft formed by these moieties of Fe^{II}PImCD is wider than that of hemoCD, MM2 calculations were carried out, and an energy-minimized structure of Fe^{II}PImCD is shown in Figure 11. Regardless of the initial structures, the calculated

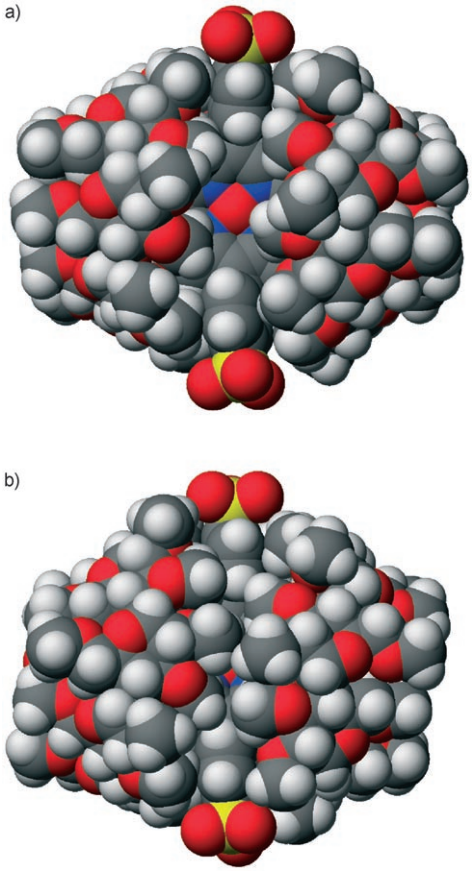

Figure 11. Energy-minimized structures of a) Fe^{II}PImCD and b) hemoCD obtained from MM2 calculations using BioMedCAChe 6.0.

structures of Fe^{II}PImCD always have wider clefts. The iron center of Fe^{II}PImCD is not hidden by two cyclodextrin moieties, whereas Fe^{II}P in hemoCD is completely encapsulated.[23,25] As mentioned above, the more-rigid and planar amide bonds in Fe^{II}PImCD inhibit the spatial contiguity of the two O-methylated cyclodextrin moieties.

Conclusions

The present study led to the following conclusions:

1) The supramolecular complex of ImCD and Fe^{II}P shows functions similar to those of Mb, namely, Fe^{II}PImCD binds dioxygen and carbon monoxide in aqueous solution.
2) The dioxygen affinity of Fe^{II}PImCD with imidazole as a single axial ligand is about 10 times higher than that of hemoCD, which has pyridine as an axial ligand.
3) The Fe^{II}PImCD system shows poorer selectivity against carbon monoxide than picket-fence porphyrins and hemoCD. The weak Fe^{II}–CO bond of CO–Fe^{II}PImCD is ascribed to the negative polar effect owing to numerous OCH_3 and OH groups surrounding the porphyrin center. CO–hemoCD has the same environment, but tight encapsulation of CO–Fe^{II}P by two cyclodextrin moieties inhibits the diffusion of dissociated CO, thus leading to higher CO selectivity.

Experimental Section

Materials

[Fe^{III}(tpps)] and [Zn^{II}(tpps)] were prepared according to the procedures described in the literature.[17c,34] The synthesis of Me-epoCD was described in a previous paper.[20] 3-(1H-imidazol-1-yl)-pentanedioic acid was synthesized according to the procedure reported in the literature.[35] The synthesis of ImCD from Me-epoCD is described below. Other chemicals were purchased and used as received. Water was purified with a Millipore Simpak 1 purification pack. Pure O_2 and N_2 (both 99.999%) gases were purchased from Sumitomo Seika Chemicals. $^{18}O_2$ and $^{13}C^{18}O$ (ICON) were used for resonance Raman spectroscopic measurements.

Syntheses

NH_2-CD: A solution of Me-epoCD (3.5 g, 2.5 mmol) in aqueous ammonia (28%, 100 mL) was stirred at 60°C for 6 h. After the solution was cooled to room temperature, ammonia gas was bubbled into the solution, which was then heated again to 60°C. After the solution was stirred at 60°C for 3 h, it was cooled to room temperature and extracted with $CHCl_3$ (3×100 mL). The organic layer was dried over Na_2SO_4, and the solvent was evaporated. The residue was purified by column chromatography on silica gel with $CHCl_3/CH_3COCH_3$ (5:2) to give NH_2-CD as a colorless solid (2.8 g, 79%). ^{1}H NMR (400 MHz, $CDCl_3$): $\delta = 5.17$–5.06 (m, 7H), 3.86–3.72 (m, 7H), 3.70–3.36 (m, 85H), 3.22–3.15 ppm (m, 7H); MS (FAB, *m*-nitrobenzyl alcohol (*m*-NBA)): *m*/*z* calcd: 1400.5 $[M+H]^+$; found: 1401.

ImCD: A mixture of 3-(1H-imidazol-1-yl)-pentanedioic acid (0.19 g, 0.95 mmol), 1-hydroxy-1H-benzotriazole (0.35 g, 2.0 mmol), and DCC (0.80 g, 3.8 mmol) in dry DMF (20 mL) was stirred at 0°C for 3 h under Ar. After the solution turned yellow-green, NH_2-CD (2.8 g, 2.0 mmol) was added to the solution, which was then stirred at room temperature for 72 h. The solvent was removed and the residue was dissolved in water (50 mL). The aqueous solution was extracted with $CHCl_3$ (3×50 mL) and the organic layer was dried over Na_2SO_4. The solvent was evaporated and the residue was purified by column chromatography on silica gel with $CHCl_3/CH_3OH$ (50:1). The residue containing the desired product was dissolved in water and dialyzed (Spectro/pro M.W.C.O. 1000) to afford pure ImCD (0.22 g, 7.8%). ^{1}H NMR (400 MHz, $CDCl_3$): $\delta = 7.67$ (s, 1H), 7.15 (s, 1H), 7.00 (s, 1H), 5.17–5.06 (m, 12H), 4.80–4.72 (m, 4H), 3.91–3.37 (m, 205H), 3.32–3.13 ppm (m, 15H); MS (FAB, *m*-NBA): *m*/*z*

calcd: 2964.2 $[M+H]^+$, 2986.1 $[M+Na]^+$; found: 2964, 2986; elemental analysis: calcd (%) for $C_{130}H_{224}O_{70}N_4 \cdot 6H_2O \cdot HCl$: C 50.24, H 7.69, O 39.13, N 1.80; found: C 49.94, H 7.26, O 38.61, N 1.84.

Measurements

UV/Vis spectra were recorded with Shimadzu UV-2100 and UV-2450 spectrophotometers with thermostatic cell holders. pH values were measured with a Horiba M-12 pH meter. ^{1}H NMR spectra were recorded with a JEOL JNM-A400 spectrometer (400 MHz). Tetramethylsilane (TMS; Nacalai) and sodium 3-trimethylsilyl[2,2,3,3-$^2H_4$]propionate (TSP; Aldrich) were used as internal (for $CDCl_3$) and external (for D_2O) standards, respectively. FAB MS spectra were recorded with a JEOL JMS-700 spectrometer. Raman scattering was performed at 413.1 nm with a Kr^+ laser (Spectra Physics, Model 2060) and detected with a charge-coupled device (CCD; Princeton Instruments, PI-CCD) attached to a single polychromator (Ritsu Oyo Kogaku, DG-1000). Mixed O_2 gas with various partial pressures in N_2 and mixed CO gas with various partial pressures in O_2 were prepared with a KOFLOC GM-4B gas-mixing apparatus (Kyoto, Japan).

Acknowledgements

This study was supported by Grants-in-Aid for Scientific Research B (No. 14340224 and 17350074) and for Scientific Research on Priority Areas (No. 16041243) from the Ministry of Education, Culture, Sports, Science, and Technology, Japan. We greatly appreciate Professor Teizo Kitagawa at Okazaki National Research Institute for his support in measuring resonance Raman spectra.

[1] a) J. P. Collman, R. Boulatov, C. J. Sunderland, L. Fu, *Chem. Rev.* **2004**, *104*, 561–588; b) T. G. Traylor, *Acc. Chem. Res.* **1981**, *14*, 102–109.
[2] a) J. P. Collman, R. R. Gagne, T. R. Halbert, J. C. Marchon, C. A. Reed, *J. Am. Chem. Soc.* **1973**, *95*, 7868–7870; b) J. P. Collman, *Acc. Chem. Res.* **1977**, *10*, 265–272.
[3] M. Momenteau, C. A. Reed, *Chem. Rev.* **1994**, *94*, 659–698.
[4] D. L. Jiang, T. Aida, *Chem. Commun.* **1996**, 1523–1524.
[5] A. Zingg, B. Felber, V. Gramlich, L. Fu, J. P. Collman, F. Diederich, *Helv. Chim. Acta* **2002**, *85*, 333–351.
[6] a) J. C. Kendrew, G. Bodo, H. M. Dintzis, R. G. Parrish, H. Wyckoff, D. C. Phillips, *Nature* **1958**, *181*, 662–666; b) J. C. Kendrew, R. E. Dickerson, B. E. Strandberg, R. G. Hart, D. R. Davis, D. C. Phillips, V. C. Shore, *Nature* **1960**, *185*, 422–427; c) J. C. Kendrew, *Science* **1963**, *139*, 1259–1266.
[7] a) M. F. Perutz, M. G. Rossmann, A. F. Cullis, H. Muirhead, G. Will, A. C. T. North, *Nature* **1960**, *185*, 416–422; b) A. F. Cullis, H. Muirhead, M. F. Perutz, M. G. Rossmann, A. C. T. North, *Proc. R. Soc. London Ser. A* **1962**, *265*, 161–187; c) M. F. Perutz, *Science* **1963**, *140*, 863–869.
[8] a) K. Shikama, *Chem. Rev.* **1998**, *98*, 1357–1373; b) K. Shikama, *Coord. Chem. Rev.* **1988**, *83*, 73–91.
[9] a) E. Tsuchida, H. Nishide, M. Yuasa, E. Hasegawa, Y. Matsushita, *J. Chem. Soc. Dalton Trans.* **1984**, 1147–1151; b) T. Komatsu, M. Moritake, A. Nakagawa, E. Tsuchida, *Chem. Eur. J.* **2002**, *8*, 5469–5480.
[10] a) T. Komatsu, N. Ohmichi, P. A. Zunszain, S. Curry, E. Tsuchida, *J. Am. Chem. Soc.* **2004**, *126*, 14304–14305; b) A. Nakagawa, N. Ohmichi, T. Komatsu, E. Tsuchida, *Org. Biomol. Chem.* **2004**, *2*, 3108–3112.
[11] E. Tsuchida, *Artificial Red Cells*, John Wiley & Sons, New York, **1995**.
[12] M. L. Bender, M. Komiyama, *Cyclodextrin Chemistry*, Springer-Verlag, New York, **1978**.
[13] C. J. Easton, S. F. Lincoln, *Modified Cyclodextrins*: *Scaffolds and Templates for Supramolecular Chemistry*, Imperial College Press, London, **1999**.
[14] R. Breslow, S. D. Dong, *Chem. Rev.* **1998**, *98*, 1997–2011.
[15] a) H. Hirai, N. Toshima, S. Hayashi, Y. Fujii, *Chem. Lett.* **1983**, 643–646; b) S. Mosseri, J. C. Mialocq, B. Perly, P. Hambright, *J. Phys. Chem.* **1991**, *95*, 2196–2203; c) S. Mosseri, J. C. Mialocq, B. Perly, P. Hambright, *J. Phys. Chem.* **1991**, *95*, 4659–4663; d) S. K. Sur, R. G. Bryant, *J. Phys. Chem.* **1995**, *99*, 7172–7179; e) S. K. Sur, R. G. Bryant, *J. Phys. Chem.* **1995**, *99*, 4900–4905; f) F. Venema, A. E. Rowan, R. J. M. Nolte, *J. Am. Chem. Soc.* **1996**, *118*, 257–258; g) S. Hamai, T. Koshiyama, *J. Photochem. Photobiol. A* **1999**, *127*, 135–141.
[16] a) J. S. Manka, D. S. Lawrence, *Tetrahedron Lett.* **1989**, *30*, 7341–7344; b) J. S. Manka, D. S. Lawrence, *J. Am. Chem. Soc.* **1990**, *112*, 2440–2442; c) D. L. Dick, T. V. S. Rao, D. Sukumaran, D. S. Lawrence, *J. Am. Chem. Soc.* **1992**, *114*, 2664–2669; d) T. Jiang, D. K. Sukumaran, S. D. Soni, D. S. Lawrence, *J. Org. Chem.* **1994**, *59*, 5149–5155; e) T. Jing, D. S. Lawrence, *J. Am. Chem. Soc.* **1995**, *117*, 1857–1858.
[17] a) K. Kano, N. Tanaka, H. Minamizono, Y. Kawakita, *Chem. Lett.* **1996**, 925–926; b) K. Kano, R. Nishiyabu, T. Asada, Y. Kuroda, *J. Am. Chem. Soc.* **2002**, *124*, 9937–9944; c) K. Kano, H. Kitagishi, S. Tamura, A. Yamada, *J. Am. Chem. Soc.* **2004**, *126*, 15202–15210; d) K. Kano, R. Nishiyabu, R. Doi, *J. Org. Chem.* **2005**, *70*, 3667–3673.
[18] T. Komatsu, S. Hayakawa, E. Tsuchida, H. Nishide, *Chem. Commun.* **2003**, 50–51.
[19] H. Zhou, J. T. Groves, *Biophys. Chem.* **2003**, *105*, 639–648.
[20] K. Kano, H. Kitagishi, M. Kodera, S. Hirota, *Angew. Chem.* **2005**, *117*, 439–442; *Angew. Chem. Int. Ed.* **2005**, *44*, 435–438.
[21] J. P. Collman, J. I. Brauman, K. M. Doxsee, J. L. Sessler, R. M. Morris, Q. H. Gibson, *Inorg. Chem.* **1983**, *22*, 1427–1432.
[22] F. Tani, M. Matsu-ura, K. Ariyama, T. Setoyama, T. Shimada, S. Kobayashi, T. Hayashi, T. Matsuo, Y. Hisaeda, Y. Naruta, *Chem. Eur. J.* **2003**, *9*, 862–870.
[23] K. Kano, H. Kitagishi, C. Dagallier, M. Kodera, T. Matsuo, T. Hayashi, Y. Hisaeda, S. Hirota, *Inorg. Chem.* **2006**, *45*, 4448–4460.
[24] K. Kalyanasundaram, *J. Chem. Soc. Faraday Trans. 2* **1983**, *79*, 1365–1374.
[25] K. Kano, H. Kitagishi, S. Tanaka, *J. Incl. Phenom. Macrocycl. Chem.*, DOI: 10.1007/s10847-006-9063-8.
[26] C. T. Watson, S. Cai, N. V. Shokhirev, F. A. Walker, *Inorg. Chem.* **2005**, *44*, 7468–7484.
[27] J. P. Collman, P. C. Herrmann, L. Fu, T. A. Eberspacher, M. Eubanks, B. Boitrel, P. Hayoz, X. Zhang, J. I. Brauman, V. W. Day, *J. Am. Chem. Soc.* **1997**, *119*, 3481–3489.
[28] a) T. Kitagawa, S. Hirota in *Handbook of Vibrational Spectroscopy* (Eds.: J. M. Chalmers, P. R. Griffiths), John Wiley & Sons, Chichester, **2002**, pp. 1–21; b) E. A. Kerr, N. T. Yu, D. E. Bartnicki, H. Mizukami, *J. Biol. Chem.* **1985**, *260*, 8360–8365; c) S. Hirota, T. Ogura, E. H. Appelman, K. Shinzawa-Itoh, S. Yoshikawa, T. Kitagawa, *J. Am. Chem. Soc.* **1994**, *116*, 10564–10570; d) M. A. Walters, T. G. Spiro, K. S. Suslick, J. P. Collman, *J. Am. Chem. Soc.* **1980**, *102*, 6857–6858.
[29] G. B. Ray, X.-Y. Li, J. A. Ibers, J. L. Sessler, T. G. Spiro, *J. Am. Chem. Soc.* **1994**, *116*, 162–176.
[30] B. A. Springer, S. G. Sligar, J. S. Olson, G. N. Phillips, Jr., *Chem. Rev.* **1994**, *94*, 699–714.
[31] J. P. Collman, J. I. Brauman, B. L. Iverson, J. L. Sessler, R. M. Morris, Q. H. Gibson, *J. Am. Chem. Soc.* **1983**, *105*, 3052–3064.
[32] M. Matsu-ura, F. Tani, Y. Naruta, *J. Am. Chem. Soc.* **2002**, *124*, 1941–1950.
[33] T. Li, M. L. Quillin, G. N. Phillips, Jr., J. S. Olson, *Biochemistry* **1994**, *33*, 1433–1446.
[34] K. Kano, S. Kobayashi, *Bull. Chem. Soc. Jpn.* **2003**, *76*, 2027–2034.
[35] S. Gil, P. Zaderenzo, F. Cruz, S. Cerdán, P. Ballesteros, *Bioorg. Med. Chem.* **1994**, *2*, 305–314.

Received: March 14, 2006
Published online: August 17, 2006

